

# Identification of Placenta Growth Factor Determinants for Binding and Activation of Flt-1 Receptor\*

Received for publication, February 9, 2004, and in revised form, June 28, 2004  
Published, JBC Papers in Press, July 21, 2004, DOI 10.1074/jbc.M401418200

Michela Errico‡§, Teresa Riccioni¶, Shalini Iyer¶, Claudio Pisano¶, K. Ravi Acharya||\*\*,  
M. Graziella Persico‡, and Sandro De Falco‡ ††

From the ‡Institute of Genetics and Biophysics “Adriano Buzzati-Traverso,” Consiglio Nazionale delle Ricerche, 80131 Naples, Italy, ¶Research and Development, Sigma-Tau SpA, Industrie Farmaceutiche Riunite, 00040 Pomezia (Rome), Italy, and the ||Department of Biology and Biochemistry, University of Bath, Bath BA2 7AY, United Kingdom

Placenta growth factor (PlGF) belongs to the vascular endothelial growth factor (VEGF) family and represents a key regulator of angiogenic events in pathological conditions. PlGF exerts its biological function through the binding and activation of the seven immunoglobulin-like domain receptor Flt-1, also known as VEGFR-1. Here, we report the first detailed mutagenesis studies that provide a basis for understanding molecular recognition between PlGF-1 and Flt-1, highlighting some of the residues that are critical for receptor recognition. Mutagenesis analysis, performed on the basis of a structural model of interaction between PlGF and the minimal binding domain of Flt-1, has led to the identification of several PlGF-1 residues involved in Flt-1 recognition. The two negatively charged residues, Asp-72 and Glu-73, located in the  $\beta$ 3– $\beta$ 4 loop, are critical for Flt-1 binding. Other mutations, which bring about a significant decrease in PlGF binding activity, are Gln-27, located in the N-terminal  $\alpha$ -helix, and Pro-98 and Tyr-100 on the  $\beta$ 6 strand. The mutation of one of the two glycosylated residues of PlGF, Asn-84, generates a PlGF variant with reduced binding activity. This indicates that, unlike in VEGF, glycosylation plays an important role in Flt-1 binding. The double mutation of residues Asp-72 and Glu-73 generates a PlGF variant unable to bind and activate the receptor molecules on the cell surface. This variant failed to induce *in vitro* capillary-like tube formation of primary endothelial cells or neo-angiogenesis in an *in vivo* chorioallantoic membrane assay.

the key regulators of pathological angiogenesis as demonstrated by gene inactivation studies (5). Human PlGF is encoded by a single gene, but alternative splicing of mature mRNA (6–8) gives rise to three known isoforms of varying length: PlGF-1 (PlGF<sub>131</sub>), PlGF-2 (PlGF<sub>152</sub>), and PlGF-3 (PlGF<sub>203</sub>). Apart from the differences in the number of amino acids, these isoforms also differ in their ability to bind heparin. The presence of a highly basic 21-amino acid insert at the C-terminal end of the protein confers upon PlGF-2 the ability to bind heparin molecules. Recently, however, a novel variant of PlGF, termed PlGF-4, was reported (9). This splice variant is believed to have the same sequence as PlGF-3 plus the heparin binding domain previously thought to be present only in PlGF-2. PlGF is secreted as a glycosylated homodimer. The most characteristic feature of PlGF is the presence of a cysteine-knot motif, consisting of an eight-residue ring formed by three intrachain and one interchain disulfide bond.

The VEGF-A homodimer exerts its biological activities through activation of two distinct tyrosine kinase receptors: *fms*-like tyrosine kinase receptor-1 (Flt-1; also known as VEGFR-1) and the kinase domain-containing receptor/fetal liver kinase receptor (KDR/Flk-1; also known as VEGFR-2) (10). VEGF-A is central to several physiological as well as pathological conditions (11, 12). The PlGF homodimer, on the other hand, binds and induces auto-phosphorylation of only Flt-1 (13). Conversely, the knockout of *Plgf* does not affect development, reproduction, or normal postnatal life but impairs angiogenesis and arteriogenesis during pathological conditions such as tumor growth, ischemic conditions, and wound healing (5, 14, 15). Synergistic cooperation between PlGF and VEGF in pathological conditions is specific (5). Up-regulation of PlGF by endothelial cells leads to displacement of VEGF from VEGFR-1. As a result, increased amounts of VEGF are available to bind to the mitogenic response-inducing receptor, VEGFR-2. Administration of recombinant PlGF amplifies VEGF-driven angiogenesis *in vivo*, stimulating the formation of mature and durable vessels in the ischemic heart and enlarging collateral arterioles in the ischemic limb with marked perfusional and functional improvement (16), without resulting in side effects such as edema and hypotension, usually observed after administration of recombinant VEGF-A (17). Furthermore, the blocking of Flt-1 activity with a neutralizing monoclonal antibody suppresses neovascularization in tumors and ischemic retina as well as in angiogenesis and inflammatory joint destruction in autoimmune arthritis (16). Altogether, these data clearly indicate that the PlGF/Flt-1 pathway plays a central role in pathological angiogenesis (5, 18).

The complexity of the biochemical relation between PlGF, VEGF-A, and the two receptors Flt-1 and Flk-1 has been explained recently, to a certain extent. Flk-1 is trans-phosphoryl-

Placenta growth factor (PlGF)<sup>1</sup> (1, 2), a member of the vascular endothelial growth factor (VEGF) family (3, 4), is one of

\* This work was supported in part by a grant from the Associazione Italiana Ricerca sul Cancro (to M. G. P.). The costs of publication of this article were defrayed in part by the payment of page charges. This article must therefore be hereby marked “advertisement” in accordance with 18 U.S.C. Section 1734 solely to indicate this fact.

§ Supported by BIOGEM scarl. Present address: CEINGE scarl, 80131 Naples, Italy.

\*\* PlGF research in this author’s laboratory was supported through Programme Grant 067288 from the Wellcome Trust, UK.

†† To whom correspondence should be addressed: Institute of Genetics and Biophysics “Adriano Buzzati-Traverso,” Consiglio Nazionale delle Ricerche, Via P. Castellino 111, 80131 Naples, Italy. Tel.: 39-081-6132354; Fax: 39-081-6132595; E-mail: defalco@igb.cnr.it.

<sup>1</sup> The abbreviations used are: PlGF, placenta growth factor; hPlGF, human PlGF; mPlGF, murine PlGF; VEGF, vascular endothelial growth factor; wt, wild type; ELISA, enzyme-linked immunosorbent assay; HUVEC, human umbilical vein endothelial cells; Erk, extracellular signal-regulated kinase; HRP, horseradish peroxidase; EBM-2, endothelial basal medium; EGM-2, endothelial growth factor-supplemented medium; RT, room temperature; PBS, phosphate-buffered saline; CAM, chorioallantoic membrane; mAb, monoclonal antibody.

ated by Flt-1 following activation by PIGF, indicating that PIGF can exert its action also through Flk-1 receptor (19). Experiments have shown that PIGF and VEGF-A form heterodimers when co-expressed within the same cell (20, 21) and induce heterodimerization of both receptors (19). The function of the PIGF/VEGF heterodimer is still under debate. Indeed, it has been shown that PIGF-1 antagonizes VEGF-driven angiogenesis and tumor growth by forming heterodimers that are functionally inactive (22). However, the recombinant PIGF/VEGF heterodimer has been successfully used to stimulate both *in vitro* and *in vivo* angiogenesis (19, 23). In addition, PIGF and VEGF-A activate Flt-1 in a different manner because only PIGF is able to stimulate the phosphorylation of specific Flt-1 tyrosine residues and to modulate the expression of distinct downstream target genes (19).

Based on the above findings, understanding the molecular details of PIGF/Flt-1 interaction becomes crucial in defining the biological role of PIGF. Despite functional diversity, the two molecules share 42% amino acid sequence identity, which in turn is reflected in the remarkable topological identity between VEGF-A and PIGF-1 (24). Recently, the three-dimensional structure of PIGF has been elucidated (25). The PIGF-1 dimer consists of two  $\alpha$ -helices and seven  $\beta$ -strands per monomer, which are covalently linked by two interchain disulfide bonds in an anti-parallel fashion. Although structural data (24, 26) and mutagenesis analysis (27) have allowed the characterization of the molecular basis of VEGF/Flt-1 interaction, no structural data were available for PIGF. The high degree of sequence identity and the availability of the crystal structure of VEGF-A in complex with domain 2 of Flt-1 (Flt-1<sub>D2</sub>) has enabled us to construct a hypothetical model in order to visualize the binding mode between PIGF and Flt-1 receptor (25).

In the present study, we report the mutational analysis of human PIGF to identify the receptor binding determinants and the role of various residues of PIGF in receptor recognition. This study allows the generation of PIGF variants that can be employed as molecular tools to eventually dissect the relationship between PIGF, VEGF-A and related receptors. While this manuscript was in preparation, the three-dimensional structure of PIGF-1 in complex with Flt-1<sub>D2</sub> was published (28). Our results are discussed taking into account the new findings.

#### EXPERIMENTAL PROCEDURES

**Materials**—Anti-human PIGF antibody, biotinylated anti-human PIGF antibody, recombinant human PIGF, and recombinant human VEGFR-1 (Flt-1/Fc chimera) were purchased from R&D Systems. Goat anti-human Flt-1, mouse anti-pY, mouse anti-pErk-1, goat anti-Erk, goat anti-mouse IgG-horseradish peroxidase (HRP), goat anti-rabbit IgG HRP, and donkey anti-goat IgG HRP were purchased from Santa Cruz Biotechnology. Matrigel™ was purchased from BD Biosciences, protein G-Sepharose 4 Fast Flow™ and the ECL Western blotting detection kit were purchased from Amersham Biosciences. Immobilon-PSQ Transfer membrane was from Millipore. Vectastain elite ABC kit was acquired from Vector Laboratories. Complete protease inhibitor mixture tablets were from Roche Applied Science. The monoclonal antibody anti-mPIGF was a gift of Dr. P. Carmeliet.

**Cell Culture and Plasmids**—HEK 293T and HEK 293 cells were grown in Dulbecco's modified Eagle's medium supplemented with 10% inactivated fetal bovine serum, 2 mM glutamine, and antibiotics. HUVEC cells (Cambrex) were grown in endothelial basal medium (EBM-2) containing endothelial growth factor supplements (EGM-2 bullet kit, Cambrex). The cDNAs coding for hPIGF-1 (29) and hFlt-1 were cloned in the pcDNA3 (Invitrogen) mammalian expression vector, and the resulting plasmids were named pchPIGF-1 and pchFlt-1, respectively.

**Construction of PIGF Variants**—Eleven PIGF variants were obtained by PCR technique using pchPIGF-1 as template and appropriate primers (available upon request). For each mutant, PCR was performed using a couple of complementary primers mapping the region encoding the amino acid to be mutated to alanine and bearing the specific nucleotide modification (QuikChange mutagenesis kit, Stratagene). For the preparation of the variant with the double mutation, primers car-

rying both mutations were utilized. Primers were designed to use the same PCR conditions: 95 °C 30 s, 1 cycle; 95 °C 30 s, 55 °C 1 min, 72 °C 12 min, 16 cycles. Then the methylated template DNA was digested with 10 units of DpnI for 60 min at 37 °C. The amplified DNA was purified and used to transform competent bacteria. In all cases, the plasmids were sequenced in both directions by the dideoxynucleotide method using SP6 and T7 standard primers. The following 10 PIGF-1 single residues were mutated to Ala: Asn-16, Pro-25, Gln-27, Cys-60, Asp-72, Glu-73, Asn-84, Pro-98, and Tyr-100. The eleventh PIGF-1 variant to be generated was the double mutant D72A/E73A.

**Transient Transfection and Selection of Stable Cell Lines**—Transient transfections were performed in the HEK 293T cell line with either pchPIGF-1 vector or the plasmids carrying the PIGF-1 variants using the calcium phosphate precipitation technique. Cells were exposed to DNA precipitate for 16 h. The precipitate was removed, and fresh medium was added. After 24 h the medium was replaced with serum-free medium followed by another 24 h of incubation after which the medium was recovered, centrifuged to eliminate cell debris, and stored at -80 °C for further analysis.

For stable transfections, the HEK 293 cells were used. After 48 h of transient expression, selection medium containing Geneticin (Invitrogen) at 0.7 mg/ml was added and replaced every 3 days. Among the isolated stable clones, the cell lines 293-hPIGF-1 (for wt PIGF-1) and 293-Q27A-PIGF-1, 293-D72A-PIGF-1, and 293-D72A/E73A-PIGF-1 (for the PIGF-1 variants) were selected for the expression of similar amount of the protein of interest, as determined by quantitative ELISAs. The 293-pcDNA3 cell line stably transfected with the empty vector was also established. The cell line 293-h-Flt-1 was selected for the maximal amount of hFlt-1 expression as determined by Western blot analysis.

**Western Blot Analysis**—Aliquots of conditioned cell media obtained from transient transfections, were precipitated overnight at -20 °C with two volumes of chilled acetone and then centrifuged at 4 °C for 30 min at 3,000 × g. The pellets were suspended in SDS loading buffer, loaded onto a nonreducing 12% SDS-PAGE, and following electrophoresis, blotted onto polyvinylidene difluoride membranes. The polyvinylidene difluoride filters were first blocked for 1 h at room temperature (RT) with 5% dried milk in TBT (25 mM Tris pH 8, 150 mM NaCl, 2.5 mM KCl, 0.1% Tween 20) and then incubated for 1 h at RT with anti-human PIGF polyclonal antibody diluted in the blocking buffer at 1 μg/ml. After three washings of 10 min each with TBT, the filter was incubated for 1 h at RT with a goat anti-rabbit antibody conjugated with HRP and diluted 1:10,000 in blocking buffer. For detection, the chemiluminescent ECL reagent was used according to the manufacturer's instructions.

**ELISAs**—For quantitative determination of PIGF-1 variants, anti-human PIGF polyclonal antibody, diluted at 1 μg/ml in PBS, pH 7.5, was used to coat a 96-well plate, 100 μl/well, overnight at 4 °C. The wells were washed five times with PBS containing 0.004% Tween 20 (PBT), and their aspecific sites were blocked for 3 h at RT with 1% bovine serum albumin in PBS, 200 μl/well. The wells were washed as described above, and recombinant PIGF, at concentrations ranging from 15.6 to 1,000 pg/ml, or the conditioned media from HEK-293T transfected with PIGF-1 variants were diluted in PBET (PBS containing 0.1% bovine serum albumin, 5 mM EDTA, 0.004% Tween 20) and incubated overnight at 4 °C. Wells were washed again, and biotinylated anti-human PIGF polyclonal antibody, diluted in PBET at 500 ng/ml, was added to the wells and incubated for 1 h at 37 °C followed by 1 h at RT. Wells were washed and incubated with a solution containing a preformed avidin and biotinylated HRP macromolecular complex (Vectastain elite ABC kit) for 1 h at RT. After the last wash, 100 μl of HRP substrate composed of 1 mg/ml of *ortho*-phenylenediamine in 50 mM citrate phosphate buffer, pH 5, 0.006% H<sub>2</sub>O<sub>2</sub> was added and incubated for 40 min in the dark at RT. The reaction was blocked by adding 30 μl/well of 4 N H<sub>2</sub>SO<sub>4</sub>, and the absorbance was measured at 490 nm on a microplate reader (Bio-Rad BenchMark). PIGF-1 variant concentrations were determined by interpolation of the standard curve using linear regression analysis.

To determine the binding activity of PIGF-1 variants to Flt-1, a 96-well plate was coated with a soluble form of human Flt-1 (Flt-1/Fc chimera) at 0.5 μg/ml in PBS, pH 7.5, 100 μl/well, overnight at RT. The plate was washed five times with PBT, and after the blocking of the aspecific sites of wells, aliquots of conditioned media were diluted in PBET and added at concentrations ranging from 1 to 100 ng/ml. The binding reaction was performed for 1 h at 37 °C and 1 h at RT. Wells were washed as described and incubated with a biotinylated anti-human PIGF polyclonal antibody, 300 ng/ml in PBET, for 1 h at 37 °C and 1 h at RT. The detection was performed as described above. All of the ELISAs reported are the means of three independent experiments.

**Flt-1 Phosphorylation Analysis**—Subconfluent 293-hFlt-1 cells were

starved overnight in serum free medium. The medium was removed, and the cell monolayer was preincubated for 5 min with 100  $\mu\text{M}$   $\text{Na}_3\text{VO}_4$  to inhibit endogenous phosphatase activity. Subsequently, cells were incubated for 10 min at 37  $^\circ\text{C}$  with wt PIGF-1 or with the PIGF variants Q27A, D72A, or D72A/E73A at concentrations ranging from 10 to 50 ng/ml. Conditioned medium from 293-pcDNA3 cells was used as control. After stimulation, cells were first washed with pre-chilled 100  $\mu\text{M}$   $\text{Na}_3\text{VO}_4$  and then lysed in a buffer containing 20 mM Tris-HCl, pH 8, 5 mM EDTA, 150 mM NaCl, 1% Triton-X100, 10% glycerol, 10 mM zinc acetate, 100  $\mu\text{M}$   $\text{Na}_3\text{VO}_4$  and a mixture of protease inhibitors for 1 h at 4  $^\circ\text{C}$ . The samples were centrifuged at 12,000  $\times g$  for 15 min, and the supernatants were recovered and stored at  $-80^\circ\text{C}$ . The protein concentration was determined by the Bradford method (Bio-Rad reagent). To immunoprecipitate Flt-1, 5  $\mu\text{g}/\text{ml}$  of a goat polyclonal antibody against human Flt-1, preincubated overnight at 4  $^\circ\text{C}$  with protein G-Sepharose, was added to 1 mg of protein extract and incubated overnight at 4  $^\circ\text{C}$ . Subsequently, the resin was recovered by centrifugation, washed once with complete lysis buffer, twice with lysis buffer without detergent, and finally with Tris-buffered saline. The pellets were loaded on a reducing 8.5% SDS-PAGE. Proteins were detected by Western blot as described above.

For the phosphotyrosine detection, mouse antibody against phosphotyrosine (anti-pY), diluted 1:1000 in blocking buffer, was used as primary antibody, and a goat anti-mouse HRP-conjugated antibody, diluted 1:10,000 in blocking buffer, was used as secondary antibody. The same filter was stripped with 0.2 N NaOH in Tris-buffered saline for 5 min at RT and used for Flt-1 detection obtained using a goat anti-human Flt-1 antibody diluted at 800 ng/ml in blocking buffer. Donkey anti-goat HRP-conjugated antibody, diluted 1:10,000 in blocking buffer, was used to detect the primary antibody.

For phospho-Erk and Erk1-2 detection, mouse anti-pErk-1 and goat anti-Erk, were used according to the manufacturer's instructions.

Densitometry analyses to quantify the degree of Flt-1 and Erk phosphorylation were performed using ImageQuant version 5.2 software (Amersham Biosciences).

**Capillary-like Tube Formation Assay**—A 24-well plate was coated with Matrigel (230  $\mu\text{l}/\text{well}$ ) for 30 min at 37  $^\circ\text{C}$ . HUVECs ( $8 \times 10^4$  cells/well) were seeded in 500  $\mu\text{l}$  of EBM-2 in the presence of either wt PIGF-1 or PIGF-1 variants at concentrations ranging from 100 to 300 ng/ml. EGM-2 and EBM-2 were used as positive and negative controls, respectively. After 6 h of incubation, capillary-like tube formation was examined under an inverted phase microscope. Cells were fixed with PBS containing 0.2% glutaraldehyde, 1% paraformaldehyde and photographed. To confirm the specificity of PIGF-1 activity, a neutralizing monoclonal antibody (2.5  $\mu\text{g}/\text{ml}$ ) was preincubated with the conditioned media containing either wt PIGF-1 or D72A/E73A-PIGF-1 variant overnight at 4  $^\circ\text{C}$ . The assays were performed in triplicate.

**Chicken Embryo Chorioallantoic Membrane (CAM) Assay**—Fertilized chicken eggs were incubated under conditions of constant humidity at 37  $^\circ\text{C}$ . On the fourth day of incubation, a window was opened in the egg shell after removal of 3–4 ml of albumen so that the developing CAM was kept detached from the shell. The window was sealed with a piece of glass, and the eggs were incubated at 37  $^\circ\text{C}$ . On the ninth day, pellets of  $3 \times 10^6$  cells of stable clones over-expressing wt PIGF-1, the PIGF-1 variants Q27A, D72A, or D72A/E73A, or the stable clone transfected with the empty vector were applied on the chorioallantoic membrane of 10 eggs for each sample. The allantoic vessels around the cell pellets were counted under a stereomicroscope and photographed with a digital camera at the time of cell implants and 72 h later.

## RESULTS

**Model-based Selection of PIGF-1 Residues Involved in Flt-1 Recognition**—The structure-based sequence alignment of PIGF and VEGF is shown in Fig. 1A. A structural model of PIGF-1/Flt-1<sub>D2</sub> interaction was built based on the three-dimensional structure of PIGF-1 (25) and the crystal structure of VEGF-A in complex with domain 2 of Flt-1 (26), the minimal domain required for binding. The model predicted a similar type of interaction as that observed for VEGF-A in that the binding is essentially driven by hydrophobic interactions. Each pole of the PIGF-1 homodimer contacts one Flt-1<sub>D2</sub> molecule, and residues from both monomers are involved in the recognition of each receptor domain. Based on this model, seven residues were chosen and mutated to alanine. Five residues, Pro-25, Gln-27, Asp-72, Glu-73, Asn-74, are located in one monomer, and the

other two residues, Pro-98 and Tyr-100, are in the other monomer (Fig. 1B). The residue Asp-72 (corresponding to Asp-63 of VEGF-A), located in the  $\beta 3$ – $\beta 4$  loop, is the only residue predicted to make a possible hydrogen-bonding interaction with Flt-1<sub>D2</sub> domain. The residue Asn-74 again located in the  $\beta 3$ – $\beta 4$  loop, the residue Gln-27 located in the N-terminal  $\alpha$ -helix, and the residue Tyr-100 located in strand  $\beta 6$  were chosen because the model predicted they would make both hydrogen-bonding and van der Waals contacts with the residues implicated in Flt-1 binding, whereas Glu-73, located in the  $\beta 3$ – $\beta 4$  loop, seems to be involved only in van der Waals interactions. The two residues Pro-25 and Pro-98, located at the beginning of the N-terminal helix and strand  $\beta 6$ , respectively, appear to be part of the interface. The residue Cys-60, involved in interchain disulfide bond formation, was mutated to verify whether the monomeric form of PIGF-1 is expressed and has the ability to bind Flt-1. In addition to the above mutations, the double mutation D72A/E73A was modeled in the crystal structures of both native PIGF-1 and PIGF-1 in complex with Flt-1<sub>D2</sub> (25) to look for possible conformational changes. Finally, the two putative glycosylation sites, Asn-16 and Asn-84, were also mutated to investigate the relationship between glycosylation and PIGF-1 activity.

**Generation of PIGF Variants**—All of the PIGF variants were generated using a PCR-based protocol and were transiently transfected in HEK 293T cells (Fig. 2). Wild type PIGF-1 and all recombinant PIGF-1 variants except N16A, N84A, and C60A showed a major band of expected molecular mass of  $\sim 46$  kDa. The two glycosylation site mutants, N16A and N84A, displayed a higher mobility, indicating that both residues are post-translationally modified. The C60A mutation determined the expression and secretion of the monomeric form of PIGF-1 with the expected molecular mass ( $\sim 23$  kDa). In some lanes, in addition to the 46-kDa band, the antibody recognized a band with mobility corresponding to the monomeric form because of over-expression by transient transfection.

**Binding of PIGF Variants to the Flt-1 Receptor**—To perform the binding of PIGF variants with the Flt-1 receptor, first the concentration of recombinant proteins in the conditioned media was determined using a sandwich ELISA. The concentration was calculated from a standard curve as reference, constructed using recombinant human PIGF. The mutants were expressed with a variable yield, and their concentrations ranged from 25 to 200 ng/ml. The binding experiments were achieved using ELISA. A fixed concentration of soluble Flt-1 receptor fused to an Fc fragment was used to coat the plate, and variable amounts of PIGF variants or wt PIGF, ranging from 0 to 16 ng/ml, were added to perform a linear binding (Fig. 3A). The interaction was evaluated using a biotinylated polyclonal antibody against hPIGF. The N16A and N74A variants showed a binding comparable with that of the wild type protein; the P25A, E73A, and Y100A variants showed a reduction of about 25% of binding, whereas Q27A, D72A, N84A, and P98A variants displayed a reduction of binding activity around 50%. The C60A variant was unable to interact with immobilized Flt-1 as expected, since residues from both the monomers of the active PIGF-1 dimer are necessary for Flt-1 recognition. Interestingly, the double mutant D72A/E73A-PIGF-1 showed a binding activity very close to that of the C60A mutant. The percentage of binding of PIGF-1 variants in comparison with the wt PIGF at a concentration of 8 ng/ml is reported in Fig. 3B.

To confirm the observations of the linear binding assay, some of the PIGF-1 variants and the wild type protein were assayed at saturating concentrations (Fig. 4A). The linear binding assay, performed with a protein concentration up to 100 ng/ml, confirmed that the variant E73A showed a reduction in binding

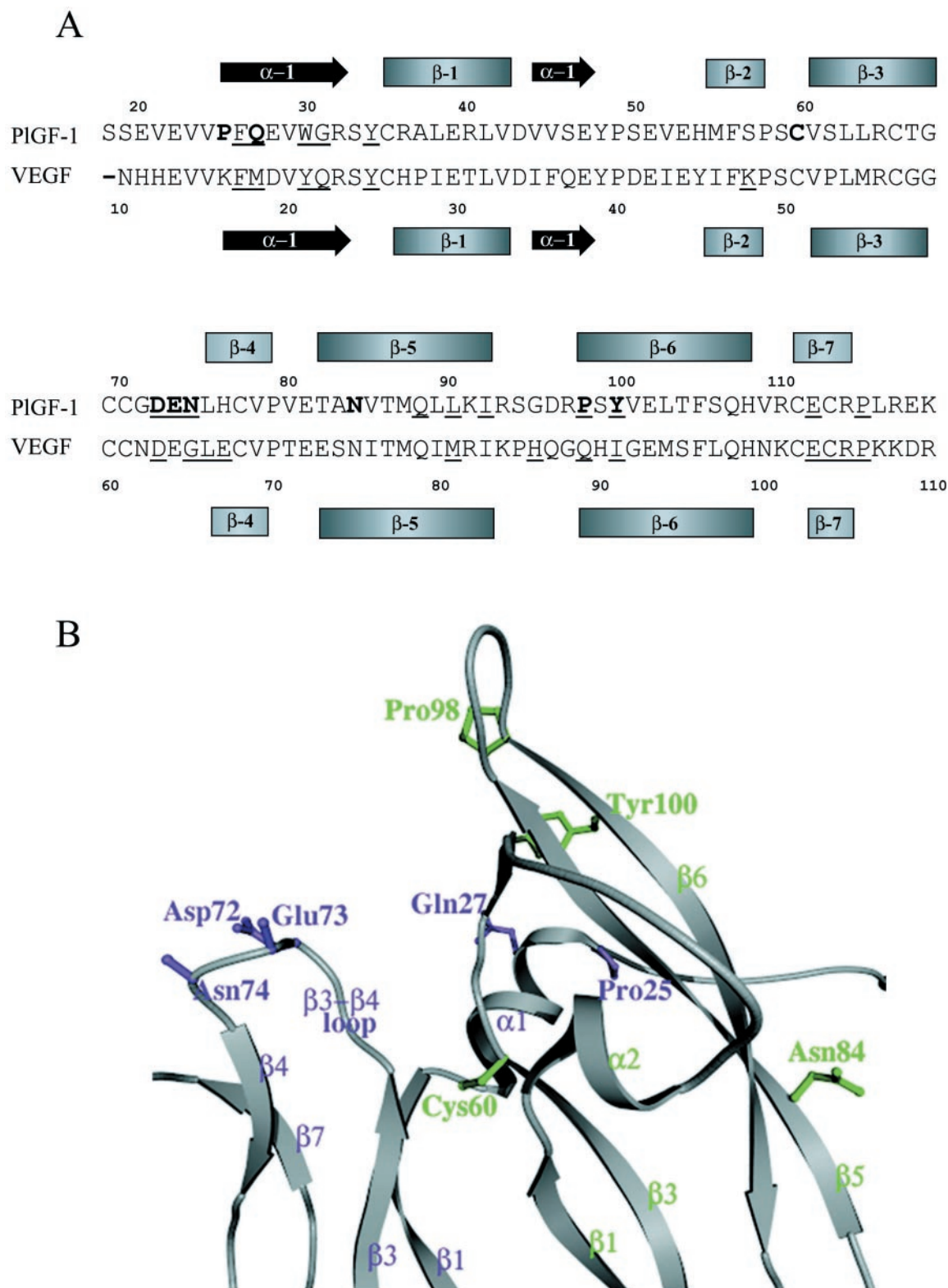


FIG. 1. *A*, structure-based sequence alignment of PlGF-1 and VEGF-A receptor binding domain. The secondary structural elements are shown as *black arrows* ( $\alpha$ -helices) and *colored bars* ( $\beta$ -strands). The residues of VEGF-A involved in Flt-1 binding are *underlined*. The PlGF-1 putative residues involved in Flt-1 binding (based on the modeling studies) are *underlined*, and the PlGF-1 residues that have been mutated are in *bold*. *B*, schematic representation of part of the PlGF-1 structure that is involved in the binding to Flt-1. The residues chosen for mutation are *ball-and-stick* representations. The residues from monomer A are shown in *blue* and those from monomer B in *green*. Glu-73 and Asn-74 were modeled as alanines in the structure of PlGF-1 (25).

of about 25%; the two variants, Q27A and D72A, displayed a binding activity close to 50% with respect to wt PlGF-1, and D72A/E73A-PlGF-1 gave a binding activity close to zero (Fig. 4B).

These results suggest that the observations derived from the

modeling studies are correct. Except for N16A and N74A residues, all mutations involved residues that contribute toward the binding of Flt-1. It is of particular relevance that the double mutation of the contiguous residues D72A and E73A generated

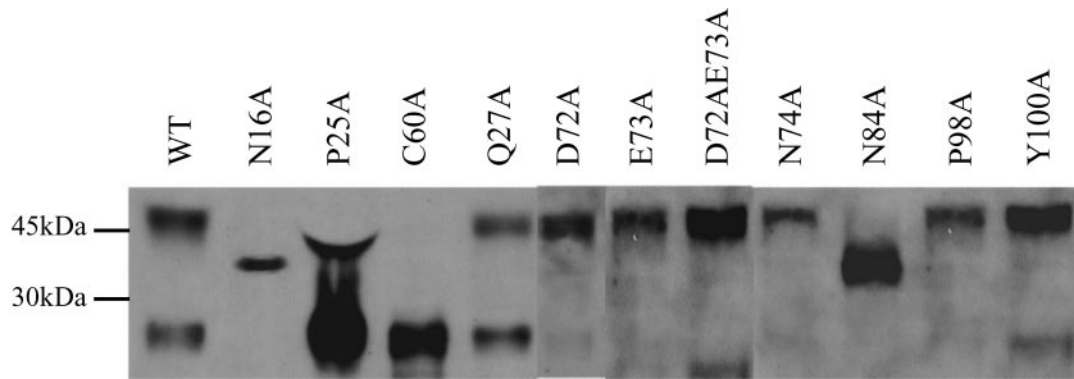


FIG. 2. **Western blot analysis of PlGF-1 variants.** Conditioned media from cells transfected with wt or mutated PlGF-1 cDNAs were loaded onto a 12% nonreducing SDS-PAGE and transferred onto a polyvinylidene difluoride membrane. The filter was probed using purified rabbit polyclonal antibody against h-PlGF-1. A band co-migrating with wt PlGF-1 dimer (46 kDa) was detected in all lanes except for the two mutants of the glycosylation sites, N16A and N84A, and the mutant that prevents dimer assembly, C60A.

a variant that severely compromised the binding of PlGF to Flt-1.

**The Double Mutant D72A/E73A-PlGF-1 Failed to Activate Flt-1**—The side-by-side, head-to-tail orientation of the PlGF-1 monomers places the receptor-binding interface at each pole of the PlGF-1 dimer. This structure facilitates receptor dimerization and, consequently, auto-phosphorylation of Flt-1, which is essential for initiating the signal transduction cascade (13). The *in vitro* data shown above indicate that the D72A/E73A-PlGF-1 mutant is unable to bind the soluble recombinant form of Flt-1, whereas the two single mutants, Q27A and D72A, show a 50% reduction of binding activity. To investigate whether this experimental evidence correlated with the inability of the double mutant to activate Flt-1 on cell surface, the stable cell line 293-Flt-1 was exposed to the wt PlGF-1 and the single or double mutant. We evaluated how these mutations affected Flt-1 phosphorylation by means of immunoprecipitation and Western blot assays. When starved 293-Flt-1 cells were incubated with 10 ng/ml PlGF-1 for 10 min (Fig. 5A, lane 2), a clear induction of Flt-1 phosphorylation with respect to the control (Fig. 5A, lane 1) was revealed using anti-phosphotyrosine antibody. Stimulation of 293-Flt-1 cells by the two single mutants Q27A-PlGF-1 and D72A-PlGF-1 (at the same concentration) resulted in Flt-1 phosphorylation at the level of 42.5 and 59.3%, respectively, when compared with that induced by wt PlGF-1 (Fig. 5A, lanes 4 and 5). When 293-Flt-1 cells were incubated with D72A/E73A-PlGF-1, no phosphorylation was detected (Fig. 5A, lane 3). These results were confirmed by the study of the activation status of the signaling proteins triggered by the receptor. Flt-1 activation determines the activation of the mitogen-activated protein kinase pathway for signal transduction (30, 31). We analyzed the activation of the extracellular signal-regulated kinase (Erk) protein in 293-Flt-1 cells after exposure to the wt or the variants of PlGF-1. To detect the phosphorylation of Erk, total cellular proteins were analyzed by Western blot using the monoclonal anti-pErk antibody and, subsequently, the anti-Erk-1 antibody for normalization. The incubation of 293-Flt-1 cells with the wild type PlGF-1 indicated phosphorylation of Erk, whereas incubation with the double mutant D72A/E73A-PlGF-1 resulted in a non-activation status of Erk, comparable with the negative control (Fig. 5B). Again, when the 293-Flt-1 cells were incubated with the two single mutants Q27A-PlGF-1 and D72A-PlGF-1, a partial activation of Erk (as compared with Erk activation by wt PlGF-1) of ~40% was detected (Fig. 5B). Taken together, these findings suggest that the residues Gln-27, Asp-72, and Glu-73 play an important role in binding and activating Flt-1. The double mutation of the residue Asp-72 and Glu-73 generated an

inactive PlGF-1 variant that failed to activate the Flt-1 signaling pathway.

**Effect of D72A/E73A-PlGF-1 on Capillary-like Tube Formation**—Cell proliferation, migration, and differentiation are processes integral to the formation of capillary-like tube structures. We examined the effect of the D72A/E73A mutation on the activity of PlGF-1 on tube formation using an *in vitro* Matrigel assay performed with human primary endothelial cells. HUVECs were plated on Matrigel and stimulated with 100 ng/ml proteins diluted in growth factor-free EBM-2 for 6 h. As a negative control, cells were incubated in EBM-2, and for positive control HUVECs were incubated in complete EGM-2 normally utilized for their *in vitro* growth.

HUVECs plated on Matrigel and stimulated with 100 ng/ml hPlGF-1 formed capillary-like networks to an extent similar to that observed for the positive control (Fig. 6, B and C), whereas stimulation with the double mutant D72A/E73A-PlGF-1 was ineffective (Fig. 6E). Increasing the concentration of the double mutant proved to be just as ineffective (data not shown). The specificity of PlGF-1 stimulation was confirmed by preincubating the wt PlGF or the D72A/E73A-PlGF-1 with a neutralizing mAb against mPlGF, at a concentration of 2.5 μg/ml. The binding of PlGF-1 to Flt-1 was completely inhibited by the neutralizing mAb as observed from the lack of response of the endothelial cells to induce capillary-like tube formation (Fig. 6, D and F), comparable with the negative control (Fig. 6A). These data indicate that the PlGF-1/Flt-1 pathway is sufficient to induce the *in vitro* organization of endothelial cells into capillary-like structures. Furthermore, the double mutant D72A/E73A-PlGF-1 was also unable to stimulate formation of capillary-like structures, similar to the inhibitory effect exerted by the neutralizing mAb on the binding of PlGF-1 to Flt-1 and the subsequent activation of the receptor.

**Mutants Q27A, D72A, and D72A/E73A Were Unable to Induce *In Vivo* Angiogenesis**—The angiogenic ability of D72A/E73A-PlGF-1 was also investigated *in vivo* by means of a CAM assay. The assay was performed using the stable cell lines 293-PlGF-1, 293-Q27A-PlGF-1, 293-D72A-PlGF-1, and 293-D72A/E73A-PlGF-1 over-expressing recombinant proteins at similar concentrations (30–40 ng/ml) as determined by quantitative ELISA. HEK-293T cells stably transfected with pCDNA3 empty vector were used as a control. A pellet of 3 × 10<sup>6</sup> cells was implanted on the embryonic chorioallantoic membrane at day 9 of incubation. After 72 h of implantation, only 293-PlGF-1 cells (Fig. 7B) were surrounded by an increased number of allantoic vessels that developed radially toward the implant, compared with 293-pCDNA3 cells (Fig. 7A), whereas no increased vascular reaction was detectable around the 293-

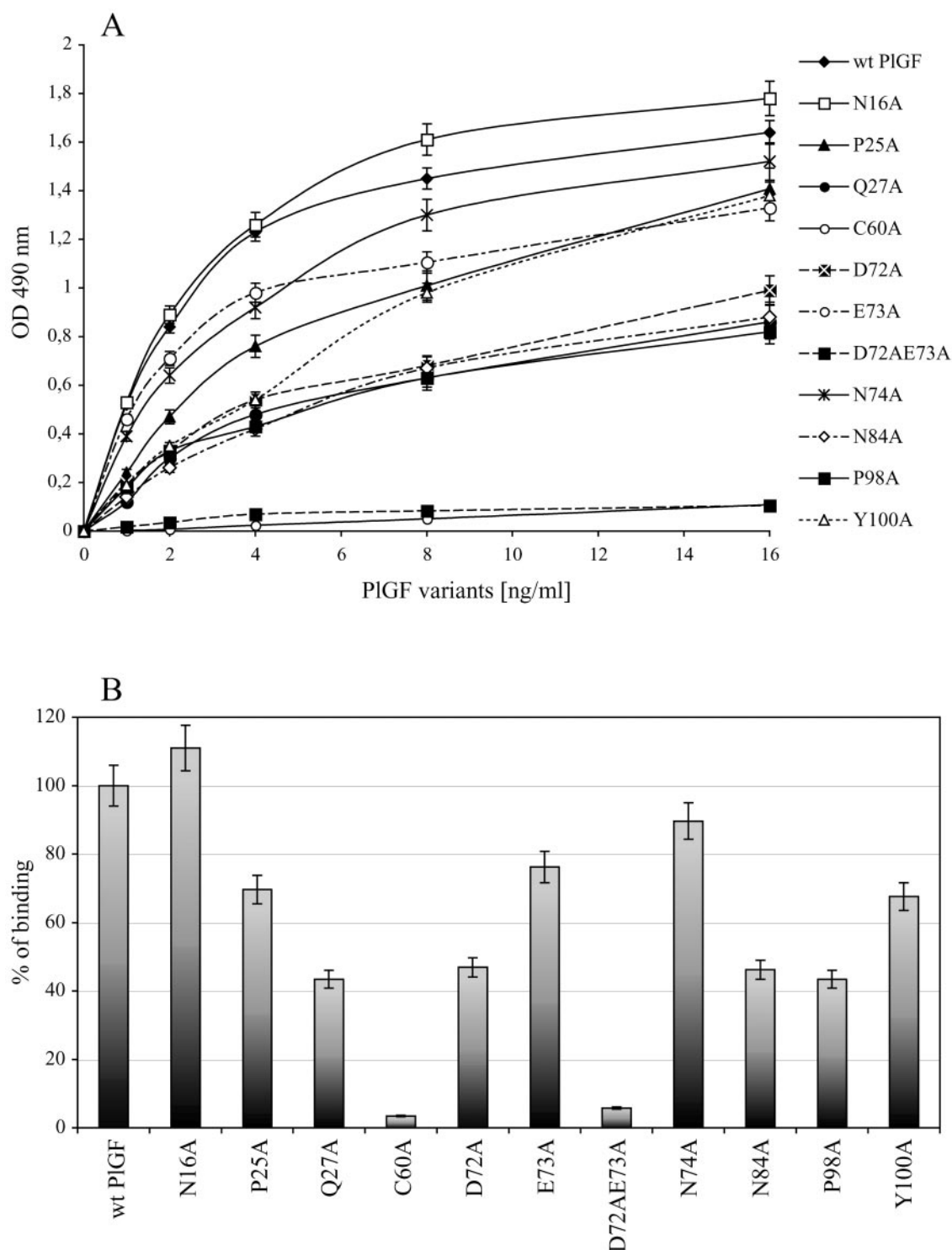


FIG. 3. ELISA-based binding of PlGF-1 variants to the soluble portion of Flt-1. A, binding of PlGF-1 variants to human Flt-1, coated at 0.5  $\mu\text{g/ml}$  on a 96-well plate, was performed using increasing concentrations of soluble proteins ranging between 1 and 16 ng/ml. Wild type PlGF-1 was used as a positive control. B, percentage of binding of PlGF-1 variants at a concentration of 8 ng/ml calculated with respect to the binding of wt PlGF-1. The results shown represent the average of three independent experiments.

Q27A-PlGF-1 (Fig. 7C), 293-D72A-PlGF-1 (Fig. 7D), and 293-D72A/E73A-PlGF-1 pellets (Fig. 7E).

Measurement of the angiogenic response, performed at day 12 of incubation, revealed that the microvessel density induced by wt PlGF-1 is comparable with that reported for VEGF-A (32). However, the double mutant D72A/E73A, as well as the two single mutants Q27A-PlGF-1 and D72A-PlGF-1, could not induce significant angiogenic response (Fig. 7F) despite their ability to partially activate Flt-1 receptor.

#### DISCUSSION

In the present study we analyzed the role of various PlGF-1 residues by means of an alanine-screening approach based on the structural model of the PlGF/Flt-1<sub>D2</sub> three-dimensional complex (25). The receptor binding activity of the different PlGF-1 variants indicates that, as seen with VEGF-A (27), the  $\beta 3$ - $\beta 4$  loop plays a crucial role in Flt-1 recognition; in particular, two residues of this loop, Asp-72 and Glu-73, are essential for interaction with the receptor. The Asp-72 residue, the only

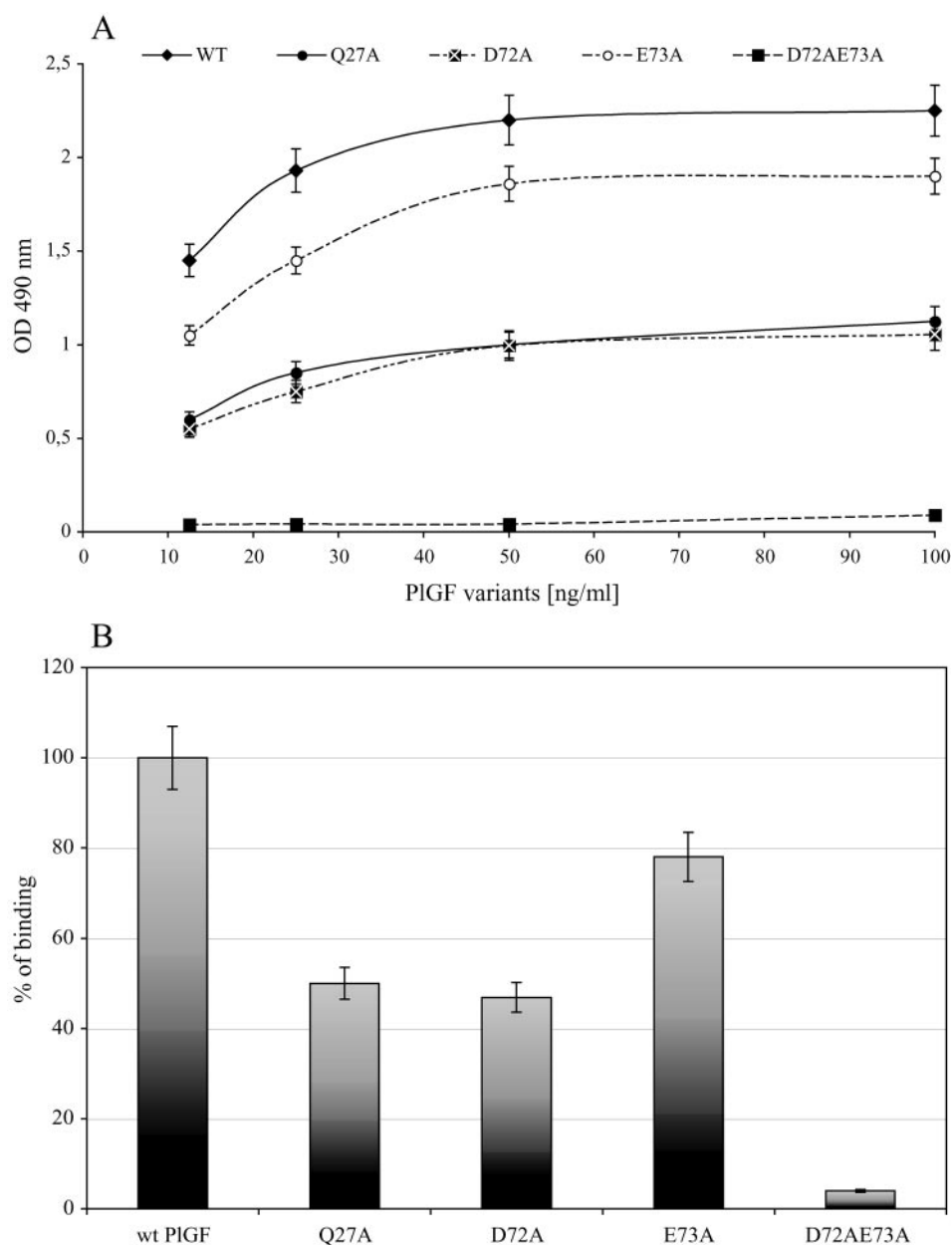


FIG. 4. **ELISA-based binding of PlGF-1 variants to Flt-1 at saturating concentrations.** A, linear binding of the Q27A, D72A, E73A, and D72A/E73A PlGF-1 variants to Flt-1 coated at 0.5  $\mu$ g/ml, performed using saturating concentrations of soluble proteins. B, percentage of binding of PlGF-1 variants at a concentration of 50 ng/ml calculated with respect to the binding of wt PlGF-1. The results shown represent the average of three independent experiments.

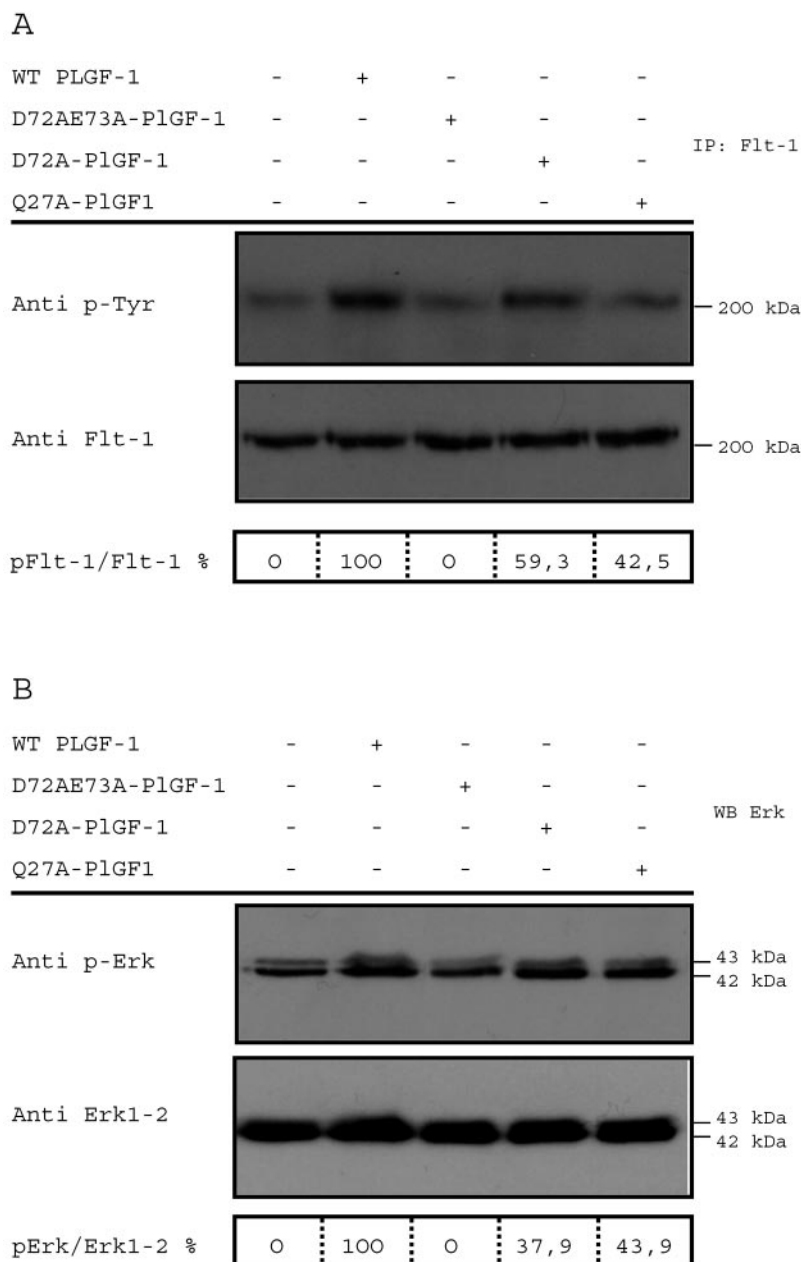
amino acid able to make direct polar interactions with Flt-1<sub>D2</sub> according to the hypothetical model, when mutated to alanine showed only about 50% receptor binding activity compared with wild type PlGF-1 (Figs. 3 and 4). Interestingly, a single mutation of the corresponding VEGF residue, Asp-63, did not give a significant decrease in receptor binding (27) indicating that perhaps Asp-72 has a more important role in Flt-1 recognition in the case of PlGF-1. Recent data from the three-dimensional crystal structure of PlGF/Flt-1<sub>D2</sub> seem to agree with our data. The authors report that Asp-72 of PlGF-1 does indeed make two polar interactions with Arg-224 of Flt-1<sub>D2</sub> (28) as hypothesized previously (25).

The single mutation of Glu-73 showed a moderate reduction of PlGF-1 binding activity (about 25%) (Figs. 3 and 4), whereas the mutation of the corresponding residue of VEGF-A (Glu-64) again did not show a significant change in receptor recognition (27). This residue, as the homologue in VEGF, is exposed to the

wide groove between the monomers and appears to be involved in the interaction with the third Ig-like domain of the receptor (25, 26). Previous data have indicated that domain 3 seems more critical for PlGF than for VEGF binding to the receptor. Alanine mutations of residues 279–283 of Flt-1 domain 3, adjacent to domain 2, resulted in a 30% reduction in bound VEGF, whereas PlGF appeared to be more sensitive to these changes, because the amount of ligand bound decreased by 60% (33). It has been recently shown that as for VEGF (26), Flt-1 domains 2 and 3 are necessary and sufficient for the binding of PlGF with near native affinity. However, the deletion of domain 3 causes only a 50-fold decrease in VEGF binding, whereas the effect on PlGF is more consistent, resulting in about a 500-fold reduction of binding of PlGF to the domain 2 (28). Thus, the mutation of residues involved in Flt-1<sub>D3</sub> interaction is more critical for PlGF than for VEGF binding.

Mutation of the two contiguous residues Asp-72 and Glu-73

**FIG. 5. Analysis of Flt-1 activation induced by wt PlGF-1 and PlGF-1 variants.** Starved 293-hFlt1 cells were stimulated with PlGF-1 and Q27A-PlGF-1, D72A-PlGF-1, and D72A/E73A PlGF-1 variants at a concentration of 10 ng/ml for 10 min. **A**, 1 mg of cell lysate was immunoprecipitated (IP) with anti-Flt1 antibodies and analyzed by Western blot, probed first with anti-phosphotyrosine antibodies (*Anti p-Tyr*), and subsequently normalized with anti-Flt1 antibodies (*Anti Flt-1*). **B**, 100  $\mu$ g of the cell protein extracts was analyzed by Western blot (WB) to reveal the phosphorylation state of the signaling protein, Erk. The blots were first immunodetected with anti-phospho-Erk antibodies (*Anti p-Erk*) and subsequently with anti-Erk1 antibodies (*Anti Erk1*). The values of densitometry analyses performed using ImageQuant 5.2 software are reported. The values of 0 and 100 have been assigned arbitrarily to non-induced and wt PlGF-1-induced samples, respectively.



to alanines resulted in the generation of a PlGF-1 variant in which binding activity was severely impaired. The mutant D72A/E73A-PlGF-1 was unable to bind Flt-1 even when saturating concentrations were used in the receptor-binding assay (Figs. 3 and 4). In VEGF-A a comparable impairment of Flt-1 recognition is obtained only when a triple mutant involving the three negatively charged residues Asp-63, Glu-64, and Glu-67 is generated (27). In PlGF-1, only the first two negatively charged amino acids are conserved (Asp-72 and Glu-73), because the third one is replaced by the positively charged amino acid His-76 (Fig. 1A). Thus, the combined mutation of the Asp-72, which makes polar interactions, and the contiguous residue Glu-73, potentially involved in Flt-1 domain 3 contact, is sufficient to generate a PlGF-1 variant that is unable to interact with Flt-1.

Although point mutations can dramatically influence both the stability and function of a protein, large or gross structural changes are rarely observed when such single/double mutations are generated. Usually the mutated residues themselves undergo conformational adaptations. The double

mutation D72A/E73A is located in the flexible, solvent-exposed  $\beta$ 3- $\beta$ 4 loop that forms an important part of the receptor-binding surface on PlGF-1. These mutations were modeled both in the native structure of PlGF-1 and the structure in complex with Flt-1<sub>D2</sub> (25) and were subjected to energy minimization in order to remove steric clashes. Superposition of these structures did not reveal any significant rearrangement of the structure in and around the mutation site. The secondary structural core of the molecule remained unperturbed. The loop containing the double mutation in the modeled mutant complex also did not show much divergence when compared with the loop in the native PlGF-1 structure (root mean square deviation of 1.1 Å for 14 C $\alpha$  atoms). The root mean square deviation value is only 0.92 Å for the same backbone atoms when the loop in the structure of the PlGF-1-Flt-1<sub>D2</sub> complex is superimposed onto that of the native PlGF-1 structure. These observations indicate that the ineffectiveness of the double mutant in all of the receptor-binding assays is not because of gross conformational change(s).

Our studies indicate that another structural element of



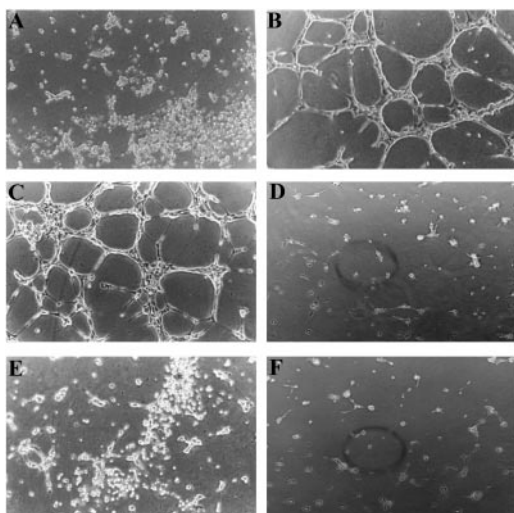


**FIG. 6. D72A/E73A-PlGF-1 variant fails to induce HUVEC capillary-like tube formation.** A, negative control performed with an amount of conditioned medium from 293 pcDNA3 comparable with that utilized in C and E, diluted in HUVEC EBM-2 medium. B, positive control performed with complete HUVEC EGM-2 medium. C, conditioned medium containing wt PlGF-1 at a concentration of 100 ng/ml. D, conditioned medium containing wt PlGF-1 at a concentration of 100 ng/ml preincubated with a cross-reacting neutralizing monoclonal antibody against mPlGF at a concentration of 2.5  $\mu$ g/ml. E, conditioned medium containing D72A/E73A-PlGF-1 at a concentration of 100 ng/ml. F, conditioned medium containing D72A/E73A-PlGF-1 at a concentration of 100 ng/ml preincubated with a cross-reacting neutralizing monoclonal antibody anti-mPlGF at a concentration of 2.5  $\mu$ g/ml. Magnification  $\times$ 10.

PlGF-1 that is critical for receptor binding is the  $\alpha$ 1-helix at the N-terminal end. We mutated the first residue of the N-terminal helix, Pro-25, and residue Gln-27, which, based on the structural model of PlGF-1/Flt-1, appears to be involved in both polar and van der Waals interactions with Flt-1<sub>D2</sub>. The variant P25A-PlGF-1 showed a limited decrease of binding activity (about 25%), whereas the Q27A-PlGF-1 variant showed a reduction of about 50% in the binding activity. The mutation data for the corresponding VEGF-A residue Met-18 or for any residue from the N-terminal  $\alpha$ 1-helix are not available, except for Arg-23, which did not show a significant reduction in affinity for Flt-1 (27). Thus, our results with the Q27A-PlGF-1 variant indicate a different role for this residue and probably for the N-terminal  $\alpha$ 1-helix in Flt-1 recognition. The recent data from the PlGF/Flt-1<sub>D2</sub> crystal structure (28) have confirmed the important role of Gln-27 in Flt-1 recognition and of the  $\alpha$ 1-helix in stabilizing the PlGF-1 dimer. The residue Gln-27 is the other PlGF-1 residue in addition to Asp-72 that is able to make polar interactions with Flt-1<sub>D2</sub>. The N-terminal helix has a fundamental role in the stabilization of the PlGF-1 dimer, because each helix packs on top of the other monomer.

Among the mutated residues, two other PlGF-1 determinants, both located on the other monomer of PlGF dimer, resulted in reduction of binding activity. The mutation of Tyr-100, which in the PlGF/Flt-1<sub>D2</sub> model is predicted to make both polar and van der Waals interactions, showed a reduction of about 25% in binding activity, whereas the mutation of Pro-98, which appears to be part of the interface and is localized at the beginning of the  $\beta$ 6 strand, showed about 50% decrease in binding activity. These results indicate that residues from the other monomer also contribute significantly to the affinity of PlGF-1 interaction with Flt-1. This finding further confirms that PlGF-1 is biologically active as a dimer, an aspect corroborated by the data obtained with the C60A-PlGF-1 variant. This mutation prevents the formation of the interchain disulfide bridge between the two PlGF-1 monomers and generates,

instead, the monomeric form. The monomer was expressed and was sufficiently stable to be secreted by the cells (Fig. 2) but was unable to bind the receptor *in vitro* (Fig. 3).

We also investigated whether glycosylation plays any role in the binding of PlGF-1 to Flt-1. PlGF-1 is glycosylated at two positions, Asn-16 and Asn-84 (Fig. 2). The mutation N16A did not modify the receptor binding activity, whereas the mutation N84A, located in the  $\beta$ 5 strand, which, according to the model of PlGF-1-Flt 1<sub>D2</sub> complex, takes part in the interaction, caused a decrease in the binding activity by about 50%. Conversely, the mutation of the corresponding residue in VEGF-A, Asn-75, did not show any reduction in binding affinity to the receptor (27). Thus, glycosylation seems to play a different role for PlGF-1 and VEGF-A in Flt-1 recognition.

With these mutation studies, we have demonstrated that the double mutation D72A/E73A is sufficient to prevent the binding of PlGF-1 to Flt-1 *in vitro*, whereas the single mutants Q27A-PlGF-1 and D72A-PlGF-1 show a 50% reduction of binding activity. The activation of the receptor is determined by the ability of PlGF-1 to induce receptor dimerization followed by auto-phosphorylation of Flt-1.

To confirm the results obtained in the ELISA-based tests, the ability of the variants Q27A-PlGF-1, D72A-PlGF-1, and D72A/E73A-PlGF-1 to induce phosphorylation of Flt-1 on the cell surface was investigated. The D72A/E73A-PlGF-1 mutant was unable to induce phosphorylation of Flt-1, whereas both of the single mutants gave an intermediate activation of Flt-1 receptor (Fig. 5A). As a consequence, the double mutant failed to activate the signaling proteins normally triggered by Flt-1 binding, whereas the partial activation of Flt-1 receptor by the single mutants resulted in a partial activation of the signaling proteins (Fig. 5B).

The inability of D72A/E73A-PlGF-1 variant to activate Flt-1 was further confirmed by two of the most common angiogenic assays, the *in vitro* capillary-like tube formation and the *in vivo* CAM assay. The double mutant was unable to induce HUVECs to organize into complex tubular structures as stimulated by wt PlGF-1. The specificity of this process was confirmed by inhibition of PlGF-1 binding to Flt-1 by means of a neutralizing monoclonal antibody (Fig. 6). Similarly, cells over-expressing the D72A/E73A-PlGF-1 variant were unable to stimulate *in vivo* neovascularization in CAM assay (Fig. 7E), whereas, as previously reported (34), wt PlGF-1 induces a significant angiogenic response (Fig. 7B). Interestingly, the cells over-expressing the single mutants Q27A-PlGF-1 and D72A-PlGF-1 failed to stimulate neovascularization in CAM assay (Fig. 7, C and D). In the same manner, both of the single mutants, despite their ability to induce a partial activation of Flt-1 receptor, were not able to induce capillary-like tube formation even when used at higher concentration (data not shown). These mutations generate PlGF variants that are unable to stimulate *in vivo* angiogenesis. These results have confirmed the ability of PlGF-1 to induce *in vitro* and *in vivo* angiogenesis and that the two residues, Asp-72 and Glu-73, of the  $\beta$ 3- $\beta$ 4 loop, as well as residue Gln-27, located in the N-terminal  $\alpha$ -helix, play a crucial role in PlGF-1-mediated angiogenic response.

The data obtained in this study have provided key information on the molecular basis of PlGF-1/Flt-1 interaction that, together with the recent crystal structure of PlGF/Flt-1<sub>D2</sub> (28), becomes essential from a therapeutic perspective. Until now, efforts to stimulate or inhibit vessel growth therapeutically have been focused primarily on VEGF-A and its receptor Flk-1 (35), but the recent developments and insights are shifting this focus on PlGF and Flt-1. PlGF is able to stimulate neo-angiogenesis at levels comparable with VEGF-A without triggering the undesired side effects, such as vascular leakage and edema,

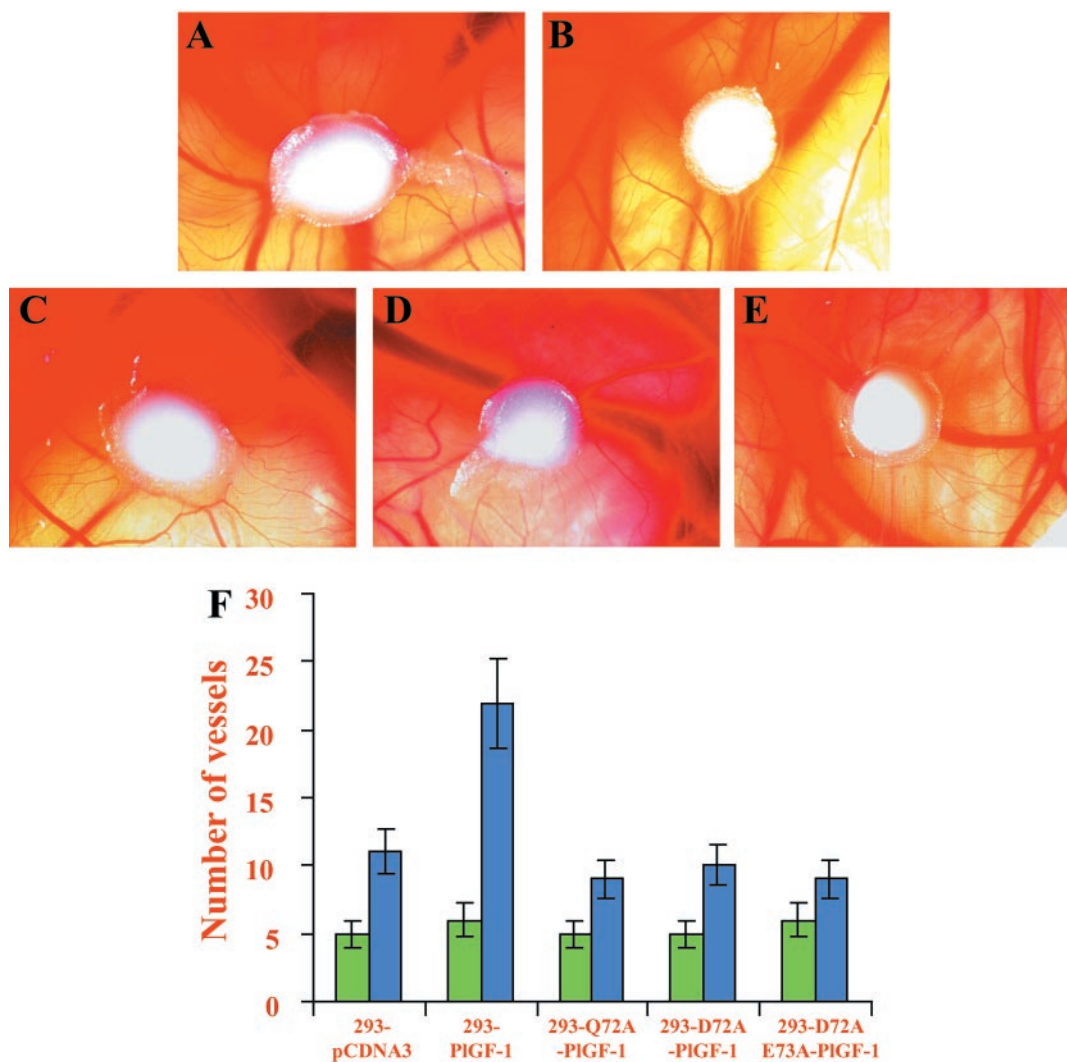


**FIG. 7. Effect of PlGF-1 variants on CAM neovascularization.** Nine-day-old chicken embryos were implanted with  $3 \times 10^6$  of 293-pCDNA3 (A), 293-PlGF-1 (B), 293-Q27A-PlGF-1 (C), 293-D72A-PlGF-1 (D), or 293-D72A/E73A-PlGF-1 cells (E). All of the stable cell lines produced comparable amounts of the protein (30–40 ng/ml). After 72 h of implantation, the new capillaries around the graft were evaluated optically by stereoscopic microscopy and photographed using a digital camera. F, vessel number at the time of the implant (green bars) and 72 h post-implantation (blue bars).

observed after administration of VEGF-A (17, 36). At the same time, a neutralizing monoclonal antibody against Flt-1 suppresses the growth of new vessels as well as angiogenesis-mediated inflammatory joint destruction in autoimmune arthritis and prevents the growth and rupture of atherosclerotic plaques (16). These results clearly indicate that PlGF and its receptor, Flt-1, represent potential therapeutic candidates for angiogenesis and inflammation (2, 18). The molecular details of PlGF/Flt-1 interaction now available could be utilized to design or to identify molecules that are able to modulate the pathway activated by the PlGF/Flt-1 interaction.

Furthermore, the D72A/E73A-PlGF-1 variant could represent a tool to investigate the role of PlGF/VEGF heterodimer. The function of the PlGF/VEGF heterodimer still remains controversial. Recently, Eriksson *et al.* (22) have reported that the PlGF/VEGF heterodimer is functionally inactive, whereas Autiero *et al.* (19) suggest that the heterodimer induces the heterodimerization of Flt-1 and Flk-1 receptors and induces an angiogenic response comparable with that of VEGF-A homodimer.

It could be hypothesized that the D72A/E73A-PlGF/VEGF heterodimer is unable to exert its biological function because of its inability to interact with the receptor on one end of the heterodimer. This heterodimer is probably unable to serve as a

molecular bridge that brings about receptor dimerization. In this perspective, a knock-in approach with the substitution of wild type PlGF with the D72A/E73A variant will generate a mouse expressing an inactive form of PlGF homodimer (comparable with the knock-out PlGF mice) but also an inactive form of PlGF/VEGF heterodimer (not present in the knock-out PlGF mice). The verification of correct embryonic development and of the response after angiogenic stimulus in the adult will help in the understanding of the role of the PlGF/VEGF heterodimer under physiological and pathological conditions.

**Acknowledgments**—We thank Dr. P. Carmeliet for the monoclonal antibody anti-mPlGF. We also thank Maria De Mol for suggestions about the ELISAs, Salvatore Ponticelli for technical assistance, and Maria D'Agostino for typing the manuscript.

#### REFERENCES

- Maglione, D., Guerriero, V., Viglietto, G., Delli-Bovi, P., and Persico, M. G. (1991) *Proc. Natl. Acad. Sci. U. S. A.* **88**, 9267–9271
- De Falco, S., Gigante, B., and Persico, M. G. (2002) *Trends Cardiovasc. Med.* **12**, 241–246
- Ferrara, N., Gerber, H. P., and LeCouter, J. (2003) *Nat. Med.* **9**, 669–676
- Yancopoulos, G. D., Davis, S., Gale, N. W., Rudge, J. S., Wiegand, S. J., and Holash, J. (2000) *Nature* **407**, 242–248
- Carmeliet, P., Moons, L., Luttun, A., Vincenzi, V., Compernelle, V., De Mol, M., Wu, Y., Bono, F., Devy, L., Beck, H., Scholz, D., Acker, T., DiPalma, T., Dewerchin, M., Noel, A., Stalmans, I., Barra, A., Blacher, S., Vanden-

- driessche, T., Ponten, A., Eriksson, U., Plate, K. H., Foidart, J. M., Schaper, W., Charnock-Jones, D. S., Hicklin, D. J., Herbert, J. M., Collen, D., and Persico, M. G. (2001) *Nat. Med.* **7**, 575–583
6. Maglione, D., Guerriero, V., Viglietto, G., Ferrara, M. G., Aprelikova, O., Alitalo, K., Del Vecchio, S., Lei, K. J., Chou, J. Y., and Persico, M. G. (1993) *Oncogene* **8**, 925–931
  7. Hauser, S., and Weich, H. A. (1993) *Growth Factors* **9**, 259–268
  8. Cao, Y., Ji, W. R., Qi, P., and Rosin, A. (1997) *Biochem. Biophys. Res. Commun.* **235**, 493–498
  9. Yang, W., Ahn, H., Hinrichs, M., Torry, R. J., and Torry, D. S. (2003) *J. Reprod. Immunol.* **60**, 53–60
  10. Sato, Y., Kanno, S., Oda, N., Abe, M., Ito, M., Shitara, K., and Shibuya, M. (2000) *Ann. N. Y. Acad. Sci.* **902**, 201–205, 205–207
  11. Ferrara, N., Carver-Moore, K., Chen, H., Dowd, M., Lu, L., O'Shea, K. S., Powell-Braxton, L., Hillan, K. J., and Moore, M. W. (1996) *Nature* **380**, 439–442
  12. Carmeliet, P., Ng, Y. S., Nuyens, D., Theilmeier, G., Brusselmans, K., Cornelissen, I., Ehler, E., Kakkar, V. V., Stalmans, I., Mattot, V., Perriard, J. C., Dewerchin, M., Flameng, W., Nagy, A., Lupu, F., Moons, L., Collen, D., D'Amore, P. A., and Shima, D. T. (1999) *Nat. Med.* **5**, 495–502
  13. Park, J. E., Chen, H. H., Winer, J., Houck, K. A., and Ferrara, N. (1994) *J. Biol. Chem.* **269**, 25646–25654
  14. Pipp, F., Heil, M., Issbrucker, K., Ziegelhoeffer, T., Martin, S., van den Heuvel, J., Weich, H., Fernandez, B., Golomb, G., Carmeliet, P., Schaper, W., and Clauss, M. (2003) *Circ. Res.* **92**, 378–385
  15. Lutun, A., Brusselmans, K., Fukao, H., Tjwa, M., Ueshima, S., Herbert, J. M., Matsuo, O., Collen, D., Carmeliet, P., and Moons, L. (2002) *Biochem. Biophys. Res. Commun.* **295**, 428–434
  16. Lutun, A., Tjwa, M., Moons, L., Wu, Y., Angelillo-Scherrer, A., Liao, F., Nagy, J. A., Hooper, A., Priller, J., De Klerck, B., Compernelle, V., Daci, E., Bohlen, P., Dewerchin, M., Herbert, J. M., Fava, R., Matthys, P., Carmeliet, G., Collen, D., Dvorak, H. F., Hicklin, D. J., and Carmeliet, P. (2002) *Nat. Med.* **8**, 831–840
  17. Thurston, G., Rudge, J. S., Ioffe, E., Zhou, H., Ross, L., Croll, S. D., Glazer, N., Holash, J., McDonald, D. M., and Yancopoulos, G. D. (2000) *Nat. Med.* **6**, 460–463
  18. Lutun, A., Tjwa, M., and Carmeliet, P. (2002) *Ann. N. Y. Acad. Sci.* **979**, 80–93
  19. Autiero, M., Waltenberger, J., Communi, D., Kranz, A., Moons, L., Lambrechts, D., Kroll, J., Plaisance, S., De Mol, M., Bono, F., Kliche, S., Fellbrich, G., Ballmer-Hofer, K., Maglione, D., Mayr-Beyrle, U., Dewerchin, M., Dombrowski, S., Stanimirovic, D., Van Hummelen, P., Dehio, C., Hicklin, D. J., Persico, G., Herbert, J. M., Shibuya, M., Collen, D., Conway, E. M., and Carmeliet, P. (2003) *Nat. Med.* **9**, 936–943
  20. DiSalvo, J., Bayne, M. L., Conn, G., Kwok, P. W., Trivedi, P. G., Soderman, D. D., Palisi, T. M., Sullivan, K. A., and Thomas, K. A. (1995) *J. Biol. Chem.* **270**, 7717–7723
  21. Cao, Y., Chen, H., Zhou, L., Chiang, M. K., Anand-Apte, B., Weatherbee, J. A., Wang, Y., Fang, F., Flanagan, J. G., and Tsang, M. L. (1996) *J. Biol. Chem.* **271**, 3154–3162
  22. Eriksson, A., Cao, R., Pawliuk, R., Berg, S. M., Tsang, M., Zhou, D., Fleet, C., Tritsarlis, K., Dissing, S., Leboulch, P., and Cao, Y. (2002) *Cancer Cell* **1**, 99–108
  23. Cao, Y., Linden, P., Shima, D., Browne, F., and Folkman, J. (1996) *J. Clin. Investig.* **98**, 2507–2511
  24. Muller, Y. A., Christinger, H. W., Keyt, B. A., and de Vos, A. M. (1997) *Structure* **5**, 1325–1338
  25. Iyer, S., Leonidas, D. D., Swaminathan, G. J., Maglione, D., Battisti, M., Tucci, M., Persico, M. G., and Acharya, K. R. (2001) *J. Biol. Chem.* **276**, 12153–12161
  26. Wiesmann, C., Fuh, G., Christinger, H. W., Eigenbrot, C., Wells, J. A., and de Vos, A. M. (1997) *Cell* **91**, 695–704
  27. Keyt, B. A., Nguyen, H. V., Berleau, L. T., Duarte, C. M., Park, J., Chen, H., and Ferrara, N. (1996) *J. Biol. Chem.* **271**, 5638–5646
  28. Christinger, H. W., Fuh, G., De Vos, A. M., and Wiesmann, C. (2004) *J. Biol. Chem.* **279**, 10382–10388
  29. Maglione, D., Guerriero, V., Rambaldi, M., Russo, G., and Persico, M. G. (1993) *Growth Factors* **8**, 141–152
  30. Desai, J., Holt-Shore, V., Torry, R. J., Caudle, M. R., and Torry, D. S. (1999) *Biol. Reprod.* **60**, 887–892
  31. Selvaraj, S. K., Giri, R. K., Perelman, N., Johnson, C., Malik, P., and Kalra, V. K. (2003) *Blood* **102**, 1515–1524
  32. Ribatti, D., Nico, B., Morbidelli, L., Donnini, S., Ziche, M., Vacca, A., Roncali, L., and Presta, M. (2001) *J. Vasc. Res.* **38**, 389–397
  33. Davis-Smyth, T., Presta, L. G., and Ferrara, N. (1998) *J. Biol. Chem.* **273**, 3216–3222
  34. Ziche, M., Maglione, D., Ribatti, D., Morbidelli, L., Lago, C. T., Battisti, M., Paoletti, I., Barra, A., Tucci, M., Parise, G., Vincenti, V., Granger, H. J., Viglietto, G., and Persico, M. G. (1997) *Lab. Investig.* **76**, 517–531
  35. Isner, J. M., Vale, P. R., Symes, J. F., and Losordo, D. W. (2001) *Circ. Res.* **89**, 389–400
  36. Epstein, S. E., Kornowski, R., Fuchs, S., and Dvorak, H. F. (2001) *Circulation* **104**, 115–119

## **Identification of Placenta Growth Factor Determinants for Binding and Activation of Flt-1 Receptor**

Michela Errico, Teresa Riccioni, Shalini Iyer, Claudio Pisano, K. Ravi Acharya, M. Graziella Persico and Sandro De Falco

*J. Biol. Chem.* 2004, 279:43929-43939.

doi: 10.1074/jbc.M401418200 originally published online July 21, 2004

---

Access the most updated version of this article at doi: [10.1074/jbc.M401418200](https://doi.org/10.1074/jbc.M401418200)

Alerts:

- [When this article is cited](#)
- [When a correction for this article is posted](#)

[Click here](#) to choose from all of JBC's e-mail alerts

This article cites 36 references, 12 of which can be accessed free at <http://www.jbc.org/content/279/42/43929.full.html#ref-list-1>